INTERNATIONAL JOURNAL FOR NUMERICAL METHODS IN FLUIDS
Int. J. Numer. Meth. Fluids 2009; **59**:1125–1155
Published online 14 July 2008 in Wiley InterScience (www.interscience.wiley.com). DOI: 10.1002/fld.1858

Numerical study of concentrated fluid–particle suspension flow in a wavy channel

S. Mukhopadhyay[1,‡], R. Usha[2,*,†] and E. G. Tulapurkara[3]

[1]*Department of Civil Engineering, Indian Institute of Technology Madras, Chennai 600 036, India*
[2]*Department of Mathematics, Indian Institute of Technology Madras, Chennai 600 036, India*
[3]*Department of Aerospace Engineering, Indian Institute of Technology Madras, Chennai 600 036, India*

SUMMARY

The particle migration effects and fluid–particle interactions occurring in the flow of highly concentrated fluid–particle suspension in a spatially modulated channel have been investigated numerically using a finite volume method. The mathematical model is based on the momentum and continuity equations for the suspension flow and a constitutive equation accounting for the effects of shear-induced particle migration in concentrated suspensions. The model couples a Newtonian stress/shear rate relationship with a shear-induced migration model of the suspended particles in which the local effective viscosity is dependent on the local volume fraction of solids. The numerical procedure employs finite volume method and the formulation is based on diffuse-flux model. Semi-implicit method for pressure linked equations has been used to solve the resulting governing equations along with appropriate boundary conditions. The numerical results are validated with the analytical expressions for concentrated suspension flow in a plane channel. The results demonstrate strong particle migration towards the centre of the channel and an increasing blunting of velocity profiles with increase in initial particle concentration. In the case of a stenosed channel, the particle concentration is lowest at the site of maximum constriction, whereas a strong accumulation of particles is observed in the recirculation zone downstream of the stenosis. The numerical procedure applied to investigate the effects of concentrated suspension flow in a wavy passage shows that the solid particles migrate from regions of high shear rate to low shear rate with low velocities and this phenomenon is strongly influenced by Reynolds numbers and initial particle concentration. Copyright © 2008 John Wiley & Sons, Ltd.

Received 12 January 2007; Revised 28 April 2008; Accepted 4 May 2008

KEY WORDS: fluid–particle suspension; finite volume method; wavy channel; lateral particle migration

*Correspondence to: R. Usha, Department of Mathematics, Indian Institute of Technology Madras, Chennai 600 036, India.
†E-mail: ushar@iitm.ac.in
‡Present address: Department of Mechanical Engineering, Indian Institute of Technology, Delhi 110 006, India.

1. INTRODUCTION

Solid–fluid suspension flows are important in a wide variety of scientific and engineering applications including the transport of sediments, chromotography, design and manufacture of composites and ceramic materials, oil and gas production, sequestration processes in porous media, environmental, physical and biological sciences. In view of its varied applications, a number of theoretical and experimental investigations have been carried out and these have explored various aspects of the flow properties and stability characteristics of suspensions. Most of the investigations on the flow properties of suspensions of spherical particles have focused their attention upon the development of theoretical or empirical formulae relating the bulk rheology to the volume fraction of particles and/or to the magnitude of the Brownian and colloidal forces, assuming that the concentration of the particles remains uniform in space. Further, the main focus in most of the investigations has been to predict the complex rheological effects on a specific suspension. These predictions are made by using the theoretical descriptions based on experimental evidence. However, it has been observed that there are a number of mechanisms that exist in the presence of the flow that leads to non-uniform concentration even in the region away from any walls or flow boundaries [1]. As a result, the volumetric flow rate for a given pressure gradient exhibits apparent non-Newtonian behaviour with a viscosity that depends on the local volume fraction of particles [2]. The transport process at a microstructural level, where the interactions between the solid particles and the carrier fluid as well as the interactions among the particles themselves play an important role, strongly influences the global physical properties of suspensions. This shows that the behaviour of the flowing suspension must be clearly understood for effectively controlling particle concentrations throughout in a variety of engineering applications such as the polymer processing industry [3–13].

The most prominent phenomenon observed in solid–fluid suspensions is shear-induced migration, in which initially well-mixed particles in suspensions subjected to inhomogeneous shear migrate from regions of high strain rate to regions of low strain rates and assume a non-uniform concentration distribution [13–19]. Shear-induced diffusion or migration has been found to be different from conventional Brownian diffusion that arises from molecular motion. This phenomenon of shear-induced migration has important implications both in viscometric measurements of concentrated suspensions (particle concentration of 30–60% by volume) and in industrial manufacturing processes, where the performances and the appearance of the finished products are greatly influenced by the degree of solids dispersivity [20]. This phenomenon also influences the process of proppant placement within hydraulic fractures that are used in the hydrocarbon extraction industry [21].

One class of effects leading to non-uniform concentration distributions in simple shear flows is the so-called ‘lateral migration’ mechanism that produces cross-stream motions of even single particles. Several mechanisms have been proposed to explain theoretically the lateral migration mechanism such as inertia, deformation of particle shape and non-Newtonian properties of the suspending liquid [18, 22]. Another source of lateral migration is due to deformation of particles as demonstrated in the case of whole blood where the particles underwent strong deformations in shape and a clear lubricating fluid (plasma) layer developed in a region near the wall in small vessels. The migration due to non-Newtonian properties of the suspending liquid has been studied by Karnis and Mason [18]. The result of the occurrence of these effects in a suspension is that the concentration profiles become non-uniform with a degree of non-uniformity that is flow-rate-dependent.

DOI: 10.1002/fld

A second class of mechanisms, recognized by Leighton and Acrivos [1], for the evolution of non-uniform concentration profiles is a consequence of irreversible hydrodynamic interactions between the neighbouring particles. They have used the flow-induced concentration non-uniformities caused by the particle interactions to explain transient stresses that have been observed when a concentrated suspension is subjected to a simple Coeutte flow. They have attributed these transients in the suspension stress to the migration of particles caused by spatial gradients in the particle interaction frequency and the particle concentration. From these arguments and simple dimensional analysis, Leightnon and Acrivos [1] have derived diffusive flux expressions for the particulate phase and have demonstrated that these are consistent with the existence of a fully developed non-uniform particle concentration distribution for flow within a parallel wall channel.

Phillips *et al.* [23] have adapted the scaling arguments of Leighton and Acrivos [1] and have derived a constitutive equation for the particle flux. The model has considered a balance between a contribution due to a spatially varying interaction frequency and a contribution due to a spatially varying viscosity and has yielded excellent predictions in a circular Couette flow. The numerical simulation of transient circular Couette flow has predicted particle migrations from the rotating inner cylinder to the stationary outer cylinder. Their results for an axisymmetric Poiseuille flow show that the particles migrate towards the centreline, leading to a sharply peaked concentration and a blunt velocity profile in that region.

A number of experimental studies have been carried out to study the effects of viscous resuspension in a pipe, a channel and Couette flow geometries [2, 14, 24–26]. The results of the experimental study of the motion of concentrated suspension in a two-dimensional channel flow for monodisperse systems by Lyon and Leal [26] show that the particle concentration distributions reach a maximum near the channel centreline and a minimum at the channel walls. Coupled to these concentration distributions are blunted velocity profiles and particle velocity fluctuation distributions that have a sharp maximum at a position approximately $0.8H\%$ from the channel axis, where H denotes half the width of the channel.

A number of theoretical models have also been developed to compute steady-state velocity and concentration profiles for flows of concentrated suspensions [23, 27–29]. These models basically fall into two categories, namely, suspension balance model and diffusive flux model, and they approximate the suspension rheology as a generalized Newtonian fluid with concentration-dependent viscosity. These models differ, however, in their approach to calculating the particle concentration distribution.

One approach is to model the suspension as an effective continuum. Suspension balance models provide a non-local description of suspension behaviour in terms of particle's velocity fluctuations and are based on statistical mechanics arguments [27, 29–31]. This approach utilizes a particulate-phase momentum balance transverse to the direction of flow, along with the recognition of a particle-phase normal stress that results from particle interactions, to obtain the equation for the particle concentration profile [27, 29–31]. Although there is no reference to the fluid in this model, the fluid does govern the nature of the interactions between particles.

The 'diffusive flux' model is based on the scaling arguments proposed by Leighton and Acrivos [1] for two-body interactions.The motion of particles within the suspension is described through a diffusion equation based on shear rate and effective viscosity gradients. In this approach, the suspension is modelled as a single continuum whereby the scaling arguments of Leighton and Acrivos [1] are used to form the basis of nonlinear constitutive model for the particle concentration

DOI: 10.1002/fld

in a flowing suspension. Particle migration and diffusion are induced by spatially varying inter-particle interaction frequency and effective viscosity. The shear-induced diffusivity scales linearly with the local shear rate. This model encounters difficulties in regions where the local shear rate approaches zero.

This continuum approach has been used for modelling a variety of flow fields and suspensions. Zhang and Acrivos [32] have considered the viscous resuspension of particles in fully developed pipe flow using finite element method for a circular cross section of the tube. Fang and Phan-Thien [33] have considered the numerical modelling of particle migration in concentrated suspension in a circular Couette flow by finite volume method.

Computer simulation of concentrated fluid–particle suspension flows in axisymmetric geometries has been performed by Hofer and Perktold [34]. The numerical procedure has employed the Galerkin finite element method and the numerical results have been validated with the analytical expression given by Phillips *et al.* [23] for steady circular tube flow. The numerical results for the case of flow through a stenosed tube model show that particle concentration is lowest at the site of maximum constriction, whereas a strong accumulation of particles has been observed in the recirculation zone downstream of the stenosis.

The experimental and theoretical investigations described above show that concentrated suspension flows in a channel, a pipe, a stenosed tube or eccentric bearing or a piston-driven flow in a tube or a channel exhibit the interesting behaviour of the migration of particles. Such a study on concentrated suspension flow through a wavy channel has not been considered so far.

It is worth mentioning here that the flow through wavy boundaries/periodic, modulated channel occurs in various physical and biological systems. The interaction between the flow field and the wavy surface produces significant changes in the transport of mass, momentum and energy. The flow is often laminar owing to the small dimensions and the low flow velocity. Wavy channels are currently used for heat transfer augmentation in practical situations. The applications range from flow in medical devices, compact heat exchangers to microelectronic equipment packages. For example, when blood oxygenators and bioreactors process very viscous liquids containing shear-sensitive biomaterials such as animal cells and plant cells, it is necessary to obtain efficient mixing and excellent heat and mass transfer characteristics. The wavy channel geometry offers an excellent alternative in these situations [35]. The Newtonian flow in a wavy channel exhibits separation, reattachment and recirculation, and the shear rate distribution differs widely from that observed in regular geometries like a plane channel or an axisymmetric tube [36]. Since flow in complex geometries, such as in modulated channels and tubes, can represent simple pore geometrical models, several experiments and numerical studies using different models and solution techniques exist for the prediction of non-Newtonian flow through complex geometries [37–44]. The interplay between inertial and non-Newtonian effects has been examined by Abu Ramadan and Khayat [45] for the flow in weakly modulated channels. The effects of modulation amplitude, wavelength, inertia and non-Newtonian behaviour and their influence on conditions of flow separation, onset of vortex flow, vortex size and location have been investigated. The results reveal that non-Newtonian effects have drastic influence and that shear-thinning leads to separation in the absence of inertia. Further, the results show a non-monotonic dependence of the vortex size on elasticity and emergence of back flow near the lower straight wall. It is observed that an increase in the wall amplitude leads to a larger vortex size and a smaller critical Reynolds number for the onset of back flow at either wall. In addition, it has been shown that the flow configuration in the converging–diverging nature of

DOI: 10.1002/fld

the periodically modulated channels provides an ideal setting for evaluating constitutive equations [38, 40, 41, 45–47] and for developing and testing the accuracy and efficiency of numerical methods in viscoelastic flow calculations [47–49]. Finite difference numerical solutions have been presented by Chiba *et al.* [50] for the flow of dilute suspensions of rigid, high aspect-ratio fibres in Newtonian fluids flowing in an axisymmetric circular 4 to 1 contraction. A continuum theory developed by Lipscomb *et al.* [51] that includes the statistical average with respect to the orientation distribution function of fibres has been used to describe the flow properties of the suspensions. The numerical results in terms of size and shape of the secondary flow vortex have been shown to be in agreement with the finite element predictions of Lipscomb *et al.* [51]. The results show that the presence of fibres drastically changes the tubular entry flow field; the salient corner vortex grows as the volume fraction and/or aspect ratio of fibres increase. Further, the vortex length decreases with an increase in the Reynolds number, due to fluid inertia.

The richness in the physical phenomena exhibited by the Newtonian/non-Newtonian flow through wavy boundaries suggests that it may be of interest to consider concentrated suspension flow in a wavy-walled channel to observe the behaviour of particle migration in it, as the migration of particles depends on the shear rate, which is a function of velocity distribution in the flow field. Such an investigation, as pointed out earlier, may be relevant for flow through biomedical devices in which the distribution of the particles in the flow has a considerable bearing on the desired flow characteristics. Further, the migration of the particles and their accumulation may lead to irreversible changes in the biofluids leading to severe consequences.

Motivated by the need to have a clear understanding of suspension flows in a wavy channel, the study of particle migration in concentrated suspension in a wavy channel has been considered. Although the study of particle migration effects in the flow of suspensions of deformable spheres in a wavy passage will be more realistic, the present study has considered the flow of suspension of rigid spheres in a wavy passage. This study is a first step towards better understanding of particle migration effects in a wavy passage. The behaviour of particle migration in concentrated suspension flow through a stenosed two-dimensional channel has been investigated. The continuum diffusive flux model has been incorporated into a finite volume method to model shear-induced particle migration in non-homogeneous shear flows of suspensions. The model couples a Newtonian stress/shear rate relationship with a shear-induced migration model of the suspended particles, with local effective viscosity depending on the local volume fraction of solids. The model describes the migration of the particles in terms of the second invariant of the generalized shear rate. The choice of diffusive flux model for the present investigation is based on the closer agreement reported by Hampton *et al.* [24]. Further, the success of finite volume method in predicting viscoelastic flow simulations in complex geometries and particle migration in concentrated suspensions [33, 52, 53] has given the confidence in the applicability of the finite volume formulation in the present study.

A general purpose code for generating a semi-staggered grid for plane geometries such as a plane channel, a stenosed channel and a wavy channel has been developed. Structured non-orthogonal grids with generalized interpolation procedures as used in finite element method have been employed. The numerical results have been validated with the analytical expression given by Phillips *et al.* [23] for a two-dimensional plane channel. The numerical procedure is then applied to a stenosed plane channel and a wavy channel, where strong variations of particle concentration occur.

DOI: 10.1002/fld

2. FORMULATION OF THE PROBLEM

2.1. Governing equations

A suspension of neutrally buoyant spherical solid particles suspended in a Newtonian fluid is considered. The flow of the concentrated suspension is assumed to be incompressible, laminar and two dimensional. The two-phase suspension of both the particles and the fluid is modelled as a single continuum. The continuity and the momentum equations for the two-dimensional suspension flow are given by

$$\frac{\partial u_i}{\partial x_i}=0 \tag{1}$$

$$\rho\left(\frac{\partial u_i}{\partial t}+u_j\frac{\partial u_i}{\partial x_j}\right)=\frac{\partial \tau_{ij}}{\partial x_j} \tag{2}$$

where ρ is the suspension mass density, $u_i (i=1,2)$ are the velocity components in the $x(=x_1)$ and $y(=x_2)$ directions, respectively, and τ_{ij} is the stress tensor. The constitutive equation for the total stress is given by the generalized Newtonian relationship

$$\tau_{ij}=-P+2\mu(\phi)D_{ij} \tag{3}$$

where P is the pressure, ϕ is the volume fraction of solids in the suspension, $\mu(\phi)$ is the effective viscosity and D_{ij} is the deformation rate tensor given by

$$D_{ij}=\frac{1}{2}\left(\frac{\partial u_i}{\partial x_j}+\frac{\partial u_j}{\partial x_i}\right) \tag{4}$$

The variation in suspension viscosity $\mu(\phi)$ with particle concentration ϕ is given as a simple correction to the solvent viscosity so that the effective suspension viscosity $\mu=\mu_r\mu_s$, where μ_s is the solvent viscosity(assumed constant) and μ_r is the relative viscosity of the suspension. Empirical correlations for the relative viscosity have been proposed by several researchers including Krieger [54] and Leighton and Acrivos [55]. In this study, Krieger's form for the viscosity function is considered and it is given by

$$\mu_r=\frac{\mu}{\mu_s}=\left(1-\frac{\phi}{\phi_m}\right)^{-1.82} \tag{5}$$

where ϕ_m is the maximum solid volume fraction for which the suspension exhibits fluid behaviour. The value of ϕ_m depends upon the uniformity of particle size, the effective microstructure of the packed configuration and the type of flow. The maximum packing fraction ϕ_m can be interpreted as the volume fraction of aggregates in closest-packing at which the effective viscosity approaches infinity. Generally, it is regarded as a variable corresponding to a given collection of particles under given conditions of flow representing the actual structure of a suspension [56]. In the present study, the maximum packing fraction is set to a value of 0.68 in the computations by considering

DOI: 10.1002/fld

only rigid monodispersed spherical particles and this is the value proposed by Phillips *et al.* [23] in their simulation of circular Coutte flow.

The particle volume fraction is governed by an evolution equation

$$\frac{\partial \phi}{\partial t} + u_i \frac{\partial \phi}{\partial x_i} = -\frac{\partial N_i}{\partial x_i} \tag{6}$$

which represents a balance between stored particles, the convected particle flux and diffusive particle flux **N**. The momentum and the concentration Equations (2)–(6) are coupled through the velocity field and concentration-dependent relative viscosity. Although several mechanisms including Brownian motion, sedimentation, hydrodynamic particle interactions and gradients in suspension viscosity contribute to the particle flux, in the present study, the diffusive particle flux is modelled by neglecting Brownian motion and assuming that sedimentation is not present due to neutral buoyancy of the particles. The flux of the particles is given by

$$\mathbf{N} = \mathbf{N}_\mu + \mathbf{N}_c \tag{7}$$

where $\mathbf{N}_\mu$ is the flux contribution due to spatial variation in viscosity, which causes a resistance to motion after a two-particle collision, and $\mathbf{N}_c$ is the flux contribution due to hydrodynamic particle interactions and it incorporates the effect of particle migration in the direction of decreasing interaction frequency $\dot{\gamma}\phi$. Both spheres are displaced in a direction of lower viscosity relative to their position in the case of no viscosity gradient. Based on the scaling arguments of Leighton and Acrivos [55], Phillips *et al.* [23] have proposed that

$$\mathbf{N}_c = -a^2 \phi K_c \nabla(\dot{\gamma}\phi) \tag{8}$$

and

$$\mathbf{N}_\mu = -a^2 \phi^2 \dot{\gamma} K_\mu \nabla(\ln \mu) \tag{9}$$

where a is the characteristic length of the particle, $\dot{\gamma}$ is the local shear rate and K_c and K_μ are proportionality constants of order 1, determined experimentally.

Although Equations (8) and (9) predict particle migration in unidirectional shear flows, it is assumed that the above model also holds in the two-dimensional case. The generalized shear rate $\dot{\gamma}$ is taken as

$$\dot{\gamma} = (2 D_{ij} D_{ij})^{1/2} \tag{10}$$

The model parameters are taken as $K_c = 0.41$ and $K_\mu = 0.62$ in accordance with the optimal values determined by Phillips *et al.* [23], based on their analysis of experimental data and numerical results. The applicability of the model in multidimensional shear flows has been supported by the investigations of Zhang and Acrivos [32] and Fang and Phan-Thien [33], who have observed a reasonable agreement between computed and experimental particle concentration in Couette flow situation. In fact, the theoretically predicted velocity and concentration profiles for flow in a circular pipe by Zhang and Acrivos [32] have been found to be in very good qualitative agreement with the experimental results reported by Altobelli *et al.* [57] where the flow velocities and particle distributions are measured by employing the technique of nuclear magnetic resonance imaging. Also, the steady-state solution in circular Couette flow obtained by Fang and Phan-Thien [33] using

DOI: 10.1002/fld

a finite volume formulation with the model described by Equations (8) and (9) is indistinguishable from the exact solutions to three significant figures (Figures 2 and 3 of Fang and Phan-Thien [33]). Further, the numerical predictions for the concentration profiles in the radial coordinates for fully two-dimensional transient flows in an eccentric bearing geometry, where the inner cylinder is placed offset from the axis of the outer cylinder, are presented along with some experimental data for a suspension of PMMA particles suspended in a density-matched liquid [33] where the data are generated by averaging the radial concentration profile with an NMR technique. The agreement is reasonable (Figures 10 and 11 of Fang and Phan-Thien [33]).

The investigations by Hofer and Perktold [34] on the flow of concentrated fluid–particle suspension flows in axisymmetric geometries using Galerkin finite element method and a velocity–pressure projection scheme generally show good agreement with the theoretical predictions (Equations (17) and (18) of Hofer and Perktold [34]). However, the particle concentration profile at the centreline has a sharp peak and this is due to the fact that the expression for the particle flux does not account for collisions in the absence of a gradient in suspension velocity; the effective shear rate $\dot{\gamma}$ is zero and the diffusive particle flux in Equations (8) and (9) opposing the migration of particles towards the centre of the tube vanishes at this site. The authors [34] have suggested the need for a further refinement of the theory as the measured particle concentration profiles in the flow experiments of Koh *et al.* [2] have been considerably smoother in the central region.

2.2. Computational domain

The computational domain for the study under consideration is a domain bounded by two rigid walls whose shape varies according to the problem under consideration. The fluid–particle suspension enters through the inlet flows through the two-dimensional domain and leaves through the outlet. For example, the computational domains for the flow through a stenosed channel and flow through a wavy passage are presented in Figures 2 and 7, respectively.

2.3. Initial and boundary conditions

The governing equations are subjected to no-slip boundary conditions ($u=0$) and the no-flux boundary condition at solid boundaries ($\hat{\mathbf{n}}\cdot\mathbf{N}=0$, where $\hat{\mathbf{n}}$ is the normal outward unit vector on the boundary). At the inlet, the flow velocity and the inlet particle volume fraction are prescribed and they vary according to the geometry and the flow under consideration. At the outflow section, the normal components of the gradients of the shear rate and the particle concentration vanish and the zero flux condition $\hat{\mathbf{n}}\cdot\mathbf{N}=0$ is satisfied. It is worth mentioning that the length of the computational domain (Figures 2, 7) has been chosen appropriately to ensure that the outlet conditions given above are satisfied. As the problem under consideration is time dependent, initial values of the flow velocities are specified. In order that the total mass of the solid phase is conserved at all times, an average volume fraction of particles over the whole domain is specified initially.

2.4. Computational scheme

The governing equations have been expressed in the form of a general transport equation

$$\frac{\partial}{\partial t}(fg)+\frac{\partial}{\partial x_j}(fu_jg)=\frac{\partial}{\partial x_j}\left(q\frac{\partial g}{\partial x_j}\right)+\delta_q \tag{11}$$

DOI: 10.1002/fld

where g represents either the velocity components or the volume fraction. When $f=1, q=0, g=\rho, \delta_q=0$, the equation of continuity (1) is recovered from Equation (11). When $f=\rho, q=\mu, g=u_i$, the momentum equation in the i direction (Equation (2)) is obtained and when $f=1, g=\phi$ and $q=a^2(k_c\phi+\phi^2 k_\mu \partial\mu/\mu\partial\phi)\dot{\gamma}$, the particle concentration equation (6) is recovered from Equation (11). The general transport Equation (11) is integrated over a finite volume Ω with the boundary surface S and this yields

$$\int_\Omega \frac{\partial}{\partial t}(fg)\mathrm{d}\Omega = \int_S f u_j g n_j \,\mathrm{d}S = \int_S q\frac{\partial g}{\partial n}\,\mathrm{d}S + \int_\Omega \delta_q \,\mathrm{d}\Omega \tag{12}$$

In this investigation, a finite volume method based on the pressure correction procedure devised by Patankar [58] and others has been employed to solve the governing equations with boundary and initial conditions numerically. The computational domain is divided into discrete control volumes using a structural non-orthogonal partially staggered mesh. The conservative form of the equations is solved for each control volume to obtain a system of algebraic equations. The resulting discretized equations for the flow variables are solved iteratively by marching in space and time. It is to be noted that in computing the gradient of any quantity ψ in a finite volume cell $\Delta\Omega$, it has been taken equal to a constant equal to its average value in the cell. This gives

$$\nabla\psi = \frac{1}{\Delta\Omega}\int_{\Delta\Omega}\nabla\psi = \frac{1}{\Delta\Omega}\int_{\Delta S}\psi\hat{n}\,\mathrm{d}S \tag{13}$$

where ΔS is the bounding surface of the cell, and $\hat{n}$ is the outward unit normal vector on ΔS.

The surface integral is evaluated using the interpolated values of ψ between adjacent cells sharing the same boundary. The numerical solution is considered to be converged when the residual for continuity and pressure defect terms are within 1×10^{-4}, and the residual of the particle flux is within 1×10^{-2}. The numerical simulations have been performed on a workstation with Pentium-IV 3 GHz processor and 1GB RAM. The code is written in C language using Microsoft Visual C++ V6.0. For post-processing of results, Microsoft Excel Tecplot V8.0 has been used.

3. VALIDITY ASSESSMENT

The numerical modelling of particle migration in concentrated suspensions by finite volume method has been considered in some simple two-dimensional geometries.

3.1. Flow between parallel plates

As a first step, the code is being validated for laminar Newtonian flow between parallel plates for Reynolds numbers of 100 and 500. A uniform velocity has been assumed at the inlet. The computed and analytical velocity profiles in fully developed regions almost coincide with each other with a maximum difference of 0.07%.

3.2. Suspension flow in a two-dimensional channel

The investigation for fully developed steady-state flow of concentrated suspension between parallel plates has been carried out to further validate the code. For Poiseuille flows of concentrated

DOI: 10.1002/fld

suspensions ($\phi_{\text{bulk}} \geqslant 0.3$), the concentration and velocity profiles reach fully developed forms. The velocity field develops faster than the concentration, and the entrance length (the length required for the corresponding variable to become fully developed) depends on the channel half width (H) and the particle radius (a). From a scaling argument, Leighton and Acrivos [1] have demonstrated that the entrance length is given by H^3/a^2. Nott and Brady [31] have obtained the same expression through dimensional analysis and Stokesian dynamic simulation. NMR experiments by Hampton *et al.* [24] have indicated that the entrance length for the velocity field is considerably less than that for the concentration, which is in turn considerably less than the estimated value H^3/a^2. Phan-Thien and Fang [52] have found these entrance lengths to be $0.2\,H^3/a^2$ and $0.5\ H^3/a^2$. The entrance lengths also depend on the ratio of particle radius to half channel width, that is, $\varepsilon = a/H$. For the flows under consideration, $\varepsilon = 0.1$ has been taken as this corresponds to the upper end of practical values and gives the minimum entrance length.

For the plane Poiseuille flow of concentrated suspension, the inlet conditions correspond to a fully developed Newtonian velocity profile with an average velocity of $u_{\text{in}} = 1\,\text{cm/s}$ and a uniform concentration at the inlet. This approach has been used in a number of studies [34, 52], as it allows development of concentration and velocity profiles in a much shorter length of channel. The parameters for the study are $Re = 500$, $a/H = 0.1$, $2H = 0.4\,\text{cm}$ and $L = 30\,\text{cm}$. The channel length taken is more than that suggested by Phan-Thien and Fang [52] to allow the development of velocity and concentration profiles. The mesh used for the numerical computations is of size 300×50. The steady solutions have been computed as time-asymptotic results of time-dependent solutions in the numerical procedure. The computations have been carried out for $\phi_{\text{inlet}} = 0.3$, 0.4 and 0.5. Figure 1 shows the computed fully developed particle concentration profiles and the velocity profiles along with the analytical solution [23, 26]. The numerical results in the channel flow demonstrate strong particle migration towards the centre of the channel and an increasing blunting of the velocity profiles with increase in initial particle concentration, which is in close agreement with the analytical solution. The computed values of ϕ at the centre are 0.645 and 0.667 for ϕ_{inlet} of 0.3 and 0.5, respectively. The analytical result shows $\phi_{\max} = 0.68$ in all three cases. This is in agreement with the results obtained by Phan-Thien and Fang [52], which shows an underprediction of ϕ at the centreline as compared with the value of $\phi_{\max}$ at the centreline. The reasons for such an underprediction can be attributed to the following. Firstly, the difficulty in the numerical computations, which arises due to viscosity tending to infinity as $\phi \to \phi_{\max}$, is overcome by arbitrarily limiting the value of ϕ to $\phi_{\max} - 0.01$. Further, the diffusivity goes to zero at the centreline, and any disturbance in concentration persists indefinitely. In order to obtain a converged solution, the dependence of kinematic fluctuations in the volume fraction is damped by an under-relaxation factor [58].

3.3. Suspension flow in a stenosed channel

A stenosed geometry is obtained by a constriction in a regular geometry like a tube or channel. A section of computational model and stenosed channel geometry are shown in Figure 2, which is based on [34].

The inlet height H of the model has been chosen as 0.4 cm and the length of the model as 50 inlet heights. The length of the stenosis region is $4H$ and the maximum area constriction is 50 or 75%. The flow Reynolds number and the ratio of particle radius to half channel width (at inlet) have been taken as $Re = 800$ and $a/H = 0.04$. A mesh of size 400×50 has been used and fully developed particle concentration profile and suspension velocity profile obtained from a flow

DOI: 10.1002/fld

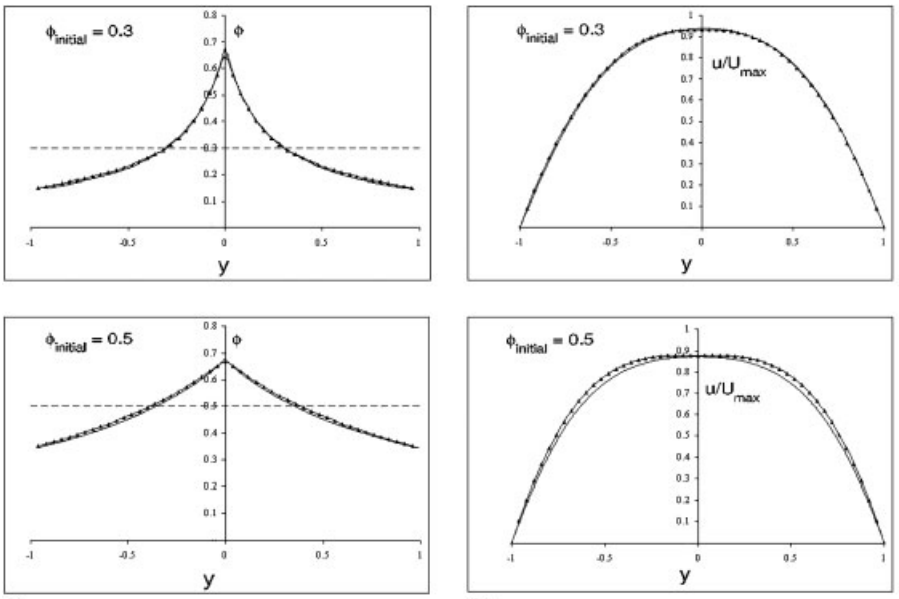

Figure 1. Comparison of analytical and numerical solutions for different values of inlet concentration: (a) particle concentration and (b) velocity profile. ——, analytical; - - - -, initial; and —$_*$—, numerical.

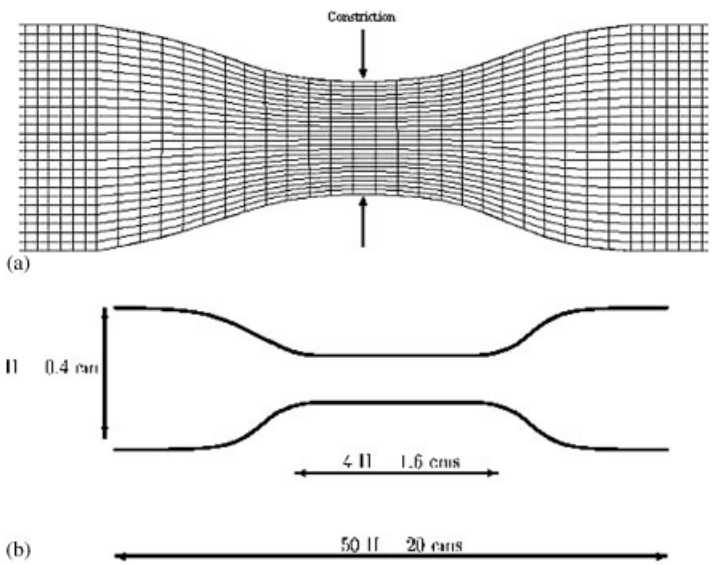

Figure 2. Schematic representation of (a) grid in the stenosed channel and (b) details of the stenosed channel.

DOI: 10.1002/fld

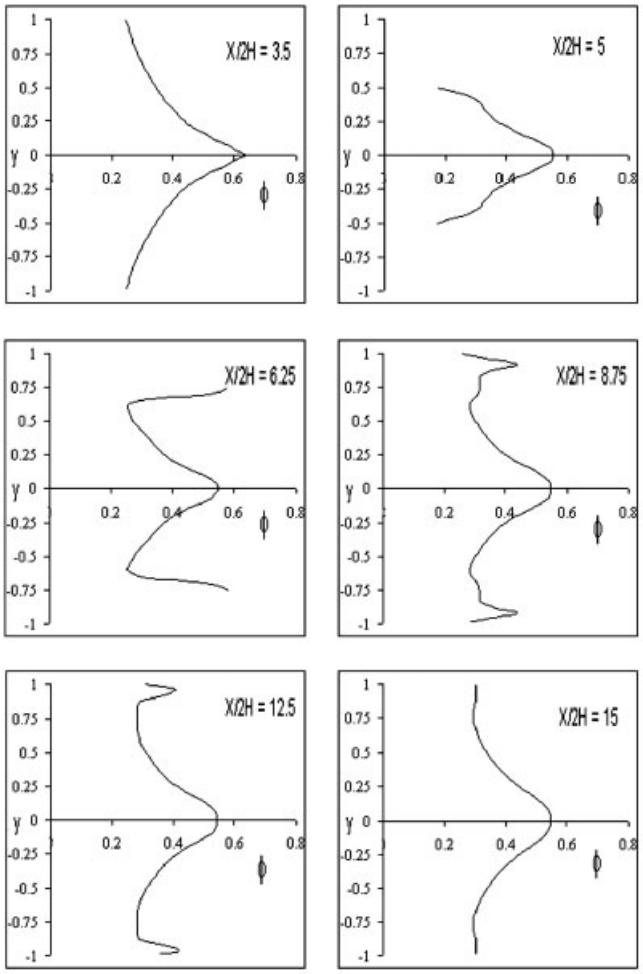

Figure 3. Concentration profiles at different locations along the length in a stenosed channel with 50% maximum area constriction for $\phi_{\text{initial}} = 0.4$.

with same ϕ_{inlet} in the plane channel model have been imposed as entrance conditions. The other boundary conditions are the same as those used in the plane channel flow.

Figures 3 and 4 show the particle concentration profiles and velocity profiles at selected lengths along the stenosed channel model for $\phi_{\text{initial}} = 0.4$ for maximum area constriction of 50%. A fully developed particle concentration profile is observed at the upstream of the stenosis, whereas at the stenosis, the area constriction gives rise to high shear rates at the wall leading to a strong migration of the particles from the wall towards the interior of the channel. The wall concentration decreases from 0.239 (Figure 3; $x/2H = 3.5$) to 0.176 (Figure 3; $x/2H = 5a$) at this site, a decrease of 26%. Near the walls, in the region downstream of the stenosis, low velocities are observed and flow separation is reflected in the corresponding concentration profile. Particle concentration in the zone

DOI: 10.1002/fld

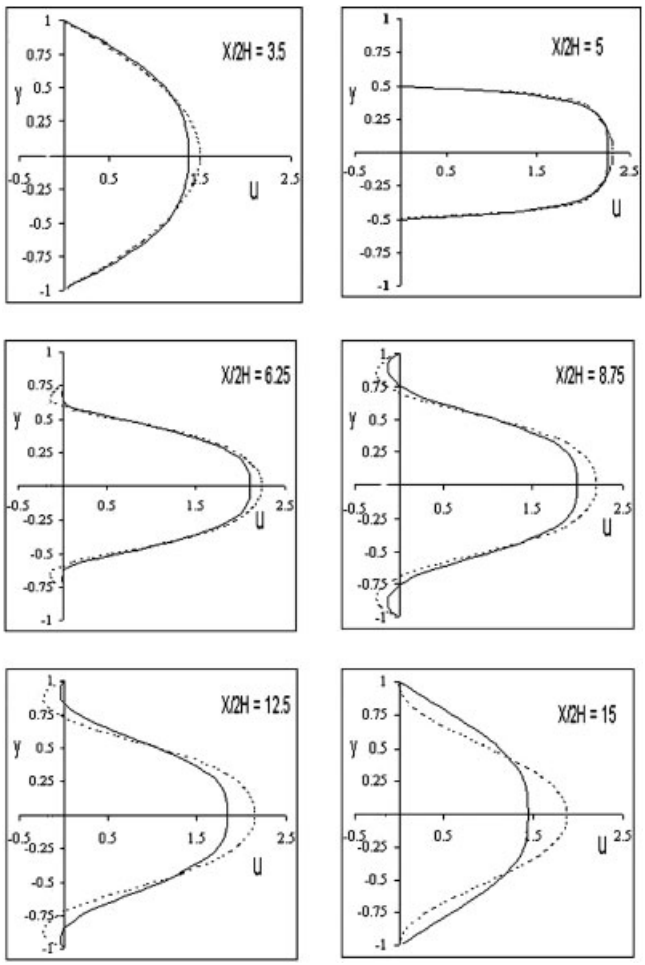

Figure 4. Comparison of velocity profiles at different locations along the length in a stenosed channel (50% maximum area constriction) for suspension flow with $\phi_{\text{initial}} = 0.4$ (solid lines) and Newtonian flow (dotted lines).

at the wall reaches a very high value of 0.581 (Figure 3; $x/2H = 6.25$). This phenomenon can be explained with the very low shear rates in the centre of the recirculation zone, which represents low collisional frequency. Further downstream the particle concentration profiles gradually transform to their fully developed shape in the channel flow. The suspension velocity profiles in the stenosed tube model exhibit higher gradients at the wall and a blunting in the centreline region when compared with Newtonian flow without particles. The recirculation is also suppressed as compared with the flow without particles.

Similar profiles are observed in the case of $\phi_{\text{initial}} = 0.5$ (Figure 5) with the concentration values being more due to a higher value of ϕ_{initial}. At maximum constriction, the concentration decreases (19% decrease) from 0.3494 (Figure 5; $x/2H = 3.5$) to 0.2843 (Figure 5; $x/2H = 5$) at the wall.

DOI: 10.1002/fld

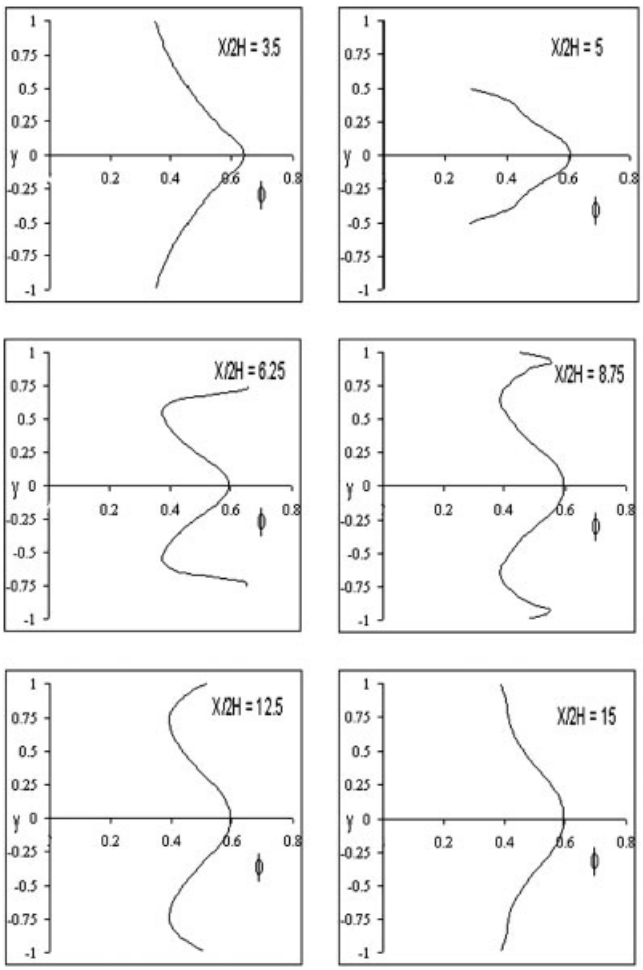

Figure 5. Concentration profiles at different locations along the length in a stenosed channel with 50% maximum area constriction for $\phi_{\text{initial}} = 0.5$.

Particle concentration at the wall in the region downstream of the stenosis is 0.651 (Figure 5; $x/2H = 6.25$), reaching almost up to the maximum packing fraction.

A higher shear rate at the wall for 50% maximum constriction is observed. As the constriction is decreased (maximum constriction limited to 75% of the channel height; Figure 6) the particle concentration distribution is similar to that in channel flow as the wall shear rate at the constriction region is not as high as in 50% maximum constriction. The particle concentration decreases from 0.24 (Figure 6; $x/2H = 3.5$) to 0.2 (Figure 6; $x/2H = 5$) in the case of $\phi_{\text{initial}} = 0.4$, a decrease of nearly 17%. A minor increase in the concentration at the wall occurs downstream of the stenosis region. The velocity profiles are blunted as compared with Newtonian flow without particles (Figure 4). It is worth mentioning that the results for suspension flow through a stenosed two-dimensional channel agree qualitatively with the particle migration behaviour in the numerical

DOI: 10.1002/fld

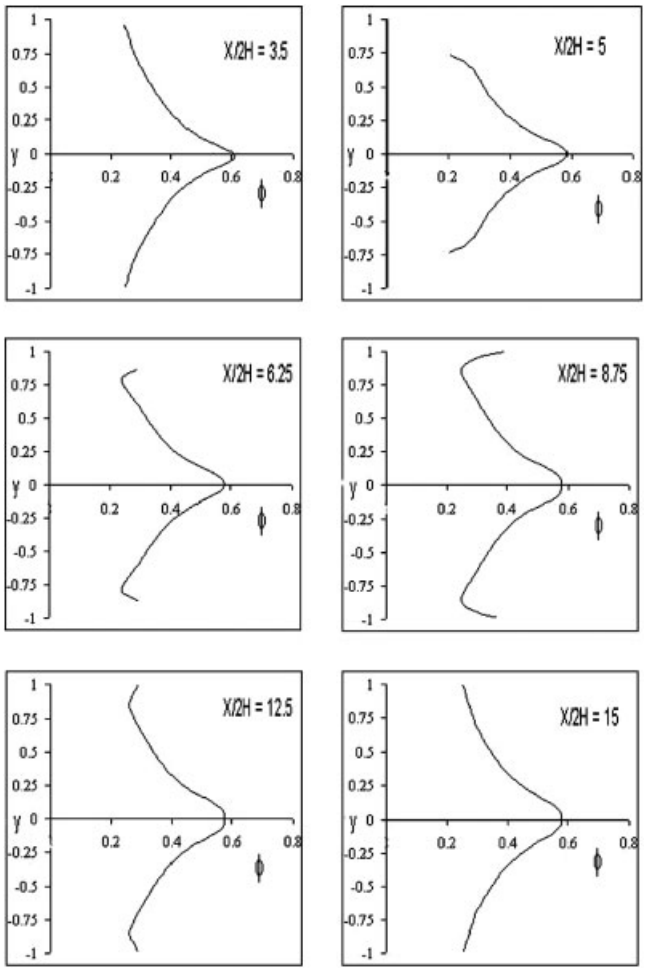

Figure 6. Concentration profiles at different locations along the length in a stenosed channel with 75% maximum area constriction for $\phi_{\text{initial}} = 0.4$.

simulations of concentrated suspension flow through a stenosed axisymmetric tube by Hofer and Perktold [34].

4. RESULTS AND DISCUSSIONS FOR A FLOW IN A WAVY CHANNEL

4.1. Newtonian model

The geometry considered for investigating the developing flow of Newtonian fluid in a wavy channel corresponds exactly to that used in the study of Stone and Vanka [36]. The wavy passage consists of 14 waves with an inlet and an outlet section with lengths each equal to that of one wavy section. The dimensions of each wavy section of the passage are identical with those used

DOI: 10.1002/fld

in the experiments of Nishimura *et al.* [59]. The schematic representation of the domain geometry and grid is shown in Figure 7. This geometry is an appropriate representation of a practical wavy channel that can be used for applications such as compact heat exchangers or biomedical devices such as blood oxygenators.

The flow is assumed to be two-dimensional and the Navier–Stokes equations governing the time-dependent flow have been solved numerically using the code developed for flow in a wavy passage. The grid size used for the computational domain in the present study is 1024×64 , which corresponds to 64×64 nodes in each wavy or straight section. The grid size is the same as used by Stone and Vanka [36] in their numerical study of developing flow and heat transfer in a wavy passage.

The flow Reynolds number is defined as $Re = u_{\text{in}} H_{\text{in}}/v$, where u_{in} and H_{in} are the velocity and height at the channel inlet, respectively. The results show that, at low Reynolds number ($Re = 120$), the flow in the wavy passage is steady, characterized by steady separation bubbles in the top and

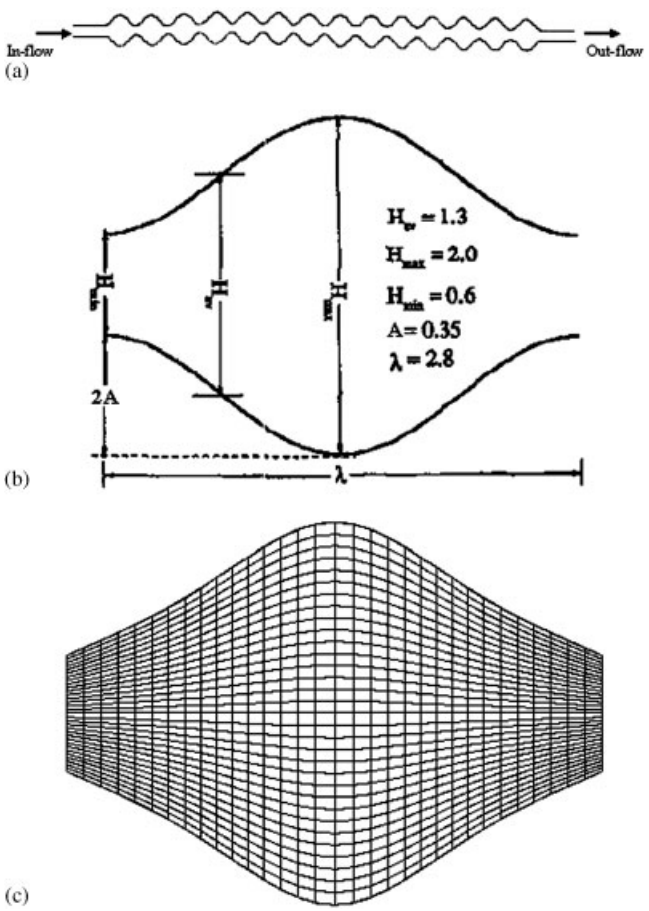

Figure 7. Schematic representation of (a) a full flow domain; (b) details of a single wavy section; and (c) computational mesh.

DOI: 10.1002/fld

bottom troughs. However, at a higher Reynolds number ($Re=300$), the flow becomes unsteady and periodic oscillations are generated. The computational results (not shown for the sake of brevity) have been observed to agree qualitatively with those presented by Stone and Vanka [36].

4.2. Concentrated suspension model

The numerical results for concentrated suspension flow in a wavy passage are presented in this section. The grid size used for computation is the same as that used for Newtonian flow through a wavy passage. In all the cases, a particle size ratio $(a/H_{\text{in}})=0.1$ has been used. The boundary conditions used are the same as those used for suspension flow in plane channel, namely, uniform axial flow (with zero cross flow) at the inlet, no-slip at the channel walls and an outflow boundary condition at the channel exit. The conditions for particle concentration are uniform concentration at the inlet and vanishing of the normal flux of particles at the walls and channel outlet. The computations have been started with an initial condition of $u=1\,\text{cm/s}$ and $\phi=\phi_{\text{initial}}$ everywhere in the computational domain. This resulted in a faster convergence to the final solution state.

It may be mentioned here that the present study on concentrated suspension flow through a wavy passage aims at investigating the behaviour of particle migration only. This has been motivated by the interesting behaviour of particle migration in concentrated suspension flow observed in different geometries, which include eccentric bearings [33], an axisymmetric pipe and a stenosed tube [34] and the plane channel [52]. The scope of the present study does not include the analysis of unsteady behaviour of concentrated suspension flow in a wavy passage. In view of this, the numerical computations have been performed for two typical values of Reynolds number ($Re=120$ and 300) and the migration of particles in the wavy passage has been observed. These values have been chosen to facilitate comparison of the velocity profiles of concentrated suspension flow with Newtonian flow (analysed in [36]).

The numerical results obtained for velocity and concentration profiles at different x locations in wave 13 have been presented in Figures 8–11 for different values of Reynolds number ($Re=120$, 300) and initial concentration values ($\phi_{\text{initial}}=0.4, 0.5$). Figures 12(a) and (b) and 13(a) and (b) present the corresponding velocity and concentration contours.

It is observed from Figures 12(a) and (b), 8 and 10 that for $Re=120$ and $\phi_{\text{initial}}=0.4$, velocity has a maximum value at the minimum cross section of the geometry, that is, at the entry to a wavy section. This is due to a sudden reduction in the flow area. As we move further downstream, the centreline velocity is considerably blunted, as compared with the Newtonian flow velocity profile. At the site of minimum area of cross section, the shear rate is higher at the wall leading to migration of the particles from the wall towards the inner section of the geometry. The concentration decreases from nearly 0.55 (at the centreline) to 0.4 (near the wall) at this site. The region downstream of the constricted portion is subject to low velocities in the central region as compared with that in the region of area reduction. Particle concentration increases slightly in this zone as compared with that in the region of area reduction. Recirculation regions are clearly seen in the velocity and concentration contour plots (Figure 12), with the particle concentration attaining a high value of 0.6 in a narrow region near the wall. The contour plot for the particle concentration in Figure 12(a) and the corresponding particle concentration profiles for $Re=120$, $\phi_{\text{initial}}=0.4$ (Figure 10) show that particles migrate out of high shear zones and concentrate in the low shear regions at the centreline and in a very narrow region near the wall where the channel height begins to increase. The recirculation region near the wall corresponds to a region of low shear rate, and consequently

DOI: 10.1002/fld

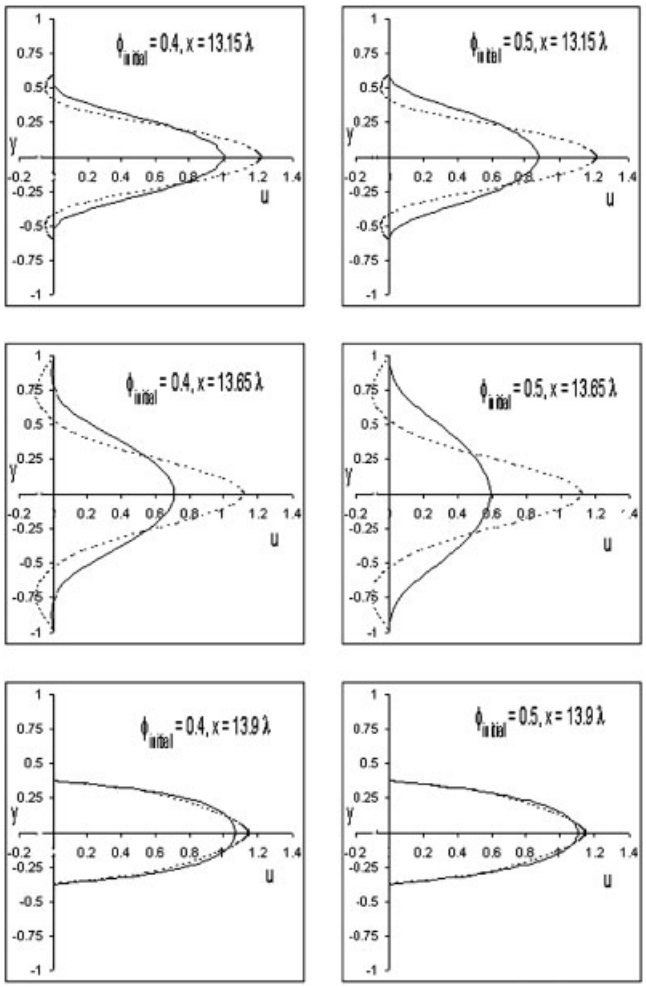

Figure 8. Comparison of axial velocity profiles for $Re = 120$ of Newtonian and suspension flow.

a local high concentration of particles is developed near this region closer to the wall. This is due to large changes in the viscosity and its gradients as a result of small changes in the particle concentration.

To gain further insight, the values of pressures in the wavy channel have been deduced from the computed results. Figure 12(d) presents the pressure contours for the entire channel and Figure 12(e) presents the details for wave 13 for the case of $Re = 120$ and $\phi = 0.4$. The corresponding contour plot for shear rate is presented in Figure 12(c). It may be pointed out that in semi-implicit method for pressure linked equations algorithm only the relative pressure is computed; the pressure at the exit of the channel is taken as zero. Figure 12(d) shows the gradual loss of pressure as the flow passes through the wavy passage. Figure 12(e) shows that pressure is uniform over the cross sections near the inlet and exit where the flow is attached. In the recirculating flow regimes, there

DOI: 10.1002/fld

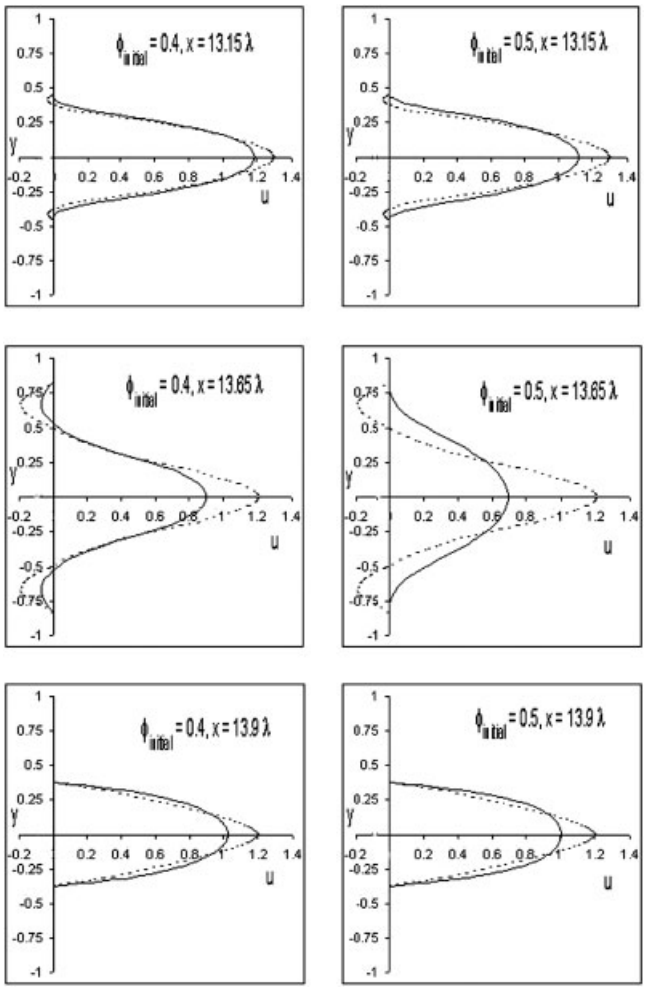

Figure 9. Comparison of axial velocity profiles for $Re = 300$ of Newtonian and suspension flow.

is loss of pressure; the velocity and shear rate are low; and there is concentration of particles. Thus, comparing Figure 12(a), (b), (c) and (d), the following picture emerges. In the regions near the entry and exit of the wave (i) the pressure is constant across the cross section, (ii) flow is attached, velocity is high in the central part, (iii) shear rate is low in the central part but high near the wall and hence (iv) the concentration is high in the central part. In the central part of the wave (i) there are regions of recirculating flow near the top and bottom, (ii) velocity, shear rate and pressure are low in the recirculating flow regimes, (iii) the velocity is maximum near the central part and hence (iv) the concentration is high in recirculating flow regions and near the centre.

It is interesting to note from Figures 13(a) and (b), 8 and 10 that for $Re = 120$, $\phi_{\text{initial}} = 0.5$, there is no recirculation zone in the troughs of the wave and there is no flow reversal in this region. This can be attributed to the high particle concentration near and at the wall in the central section

DOI: 10.1002/fld

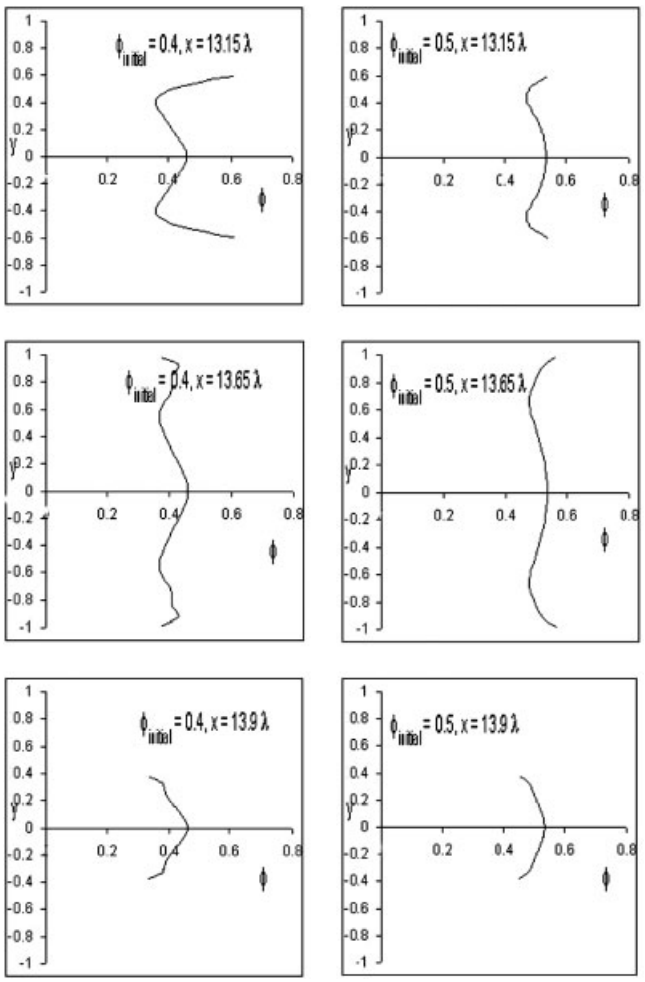

Figure 10. Concentration profiles of suspension flow for $Re = 120$.

of the wave as compared with particle concentration in this region when $\phi_{\text{initial}} = 0.4$ for the same Reynolds number. The increase in the initial particle concentration ($\phi_{\text{initial}} = 0.5$) suppresses the recirculation in the troughs of the wave. In these regions, the particle concentration takes a high value of 0.574. The results predict increased blunting of the velocity profiles with the increase in ϕ_{initial} from 0.4 to 0.5. The contour plots of shear rates are shown in Figure 14 and they explain the particle concentration contours in Figure 13(a). The very low shear rates in the troughs (Figure 14), which represents a region of low collisional frequency, lead to high particle concentration in the wave troughs. This phenomenon is also observed in the region closer to the wall where the channel height increases. Further downstream along the wall, the particle concentration again increases.

With increase in Reynolds number to $Re = 300$, it is observed from Figures 12(a) and (b), 9 and 11 that the recirculation takes place in the entire region of the troughs of the wave when

DOI: 10.1002/fld

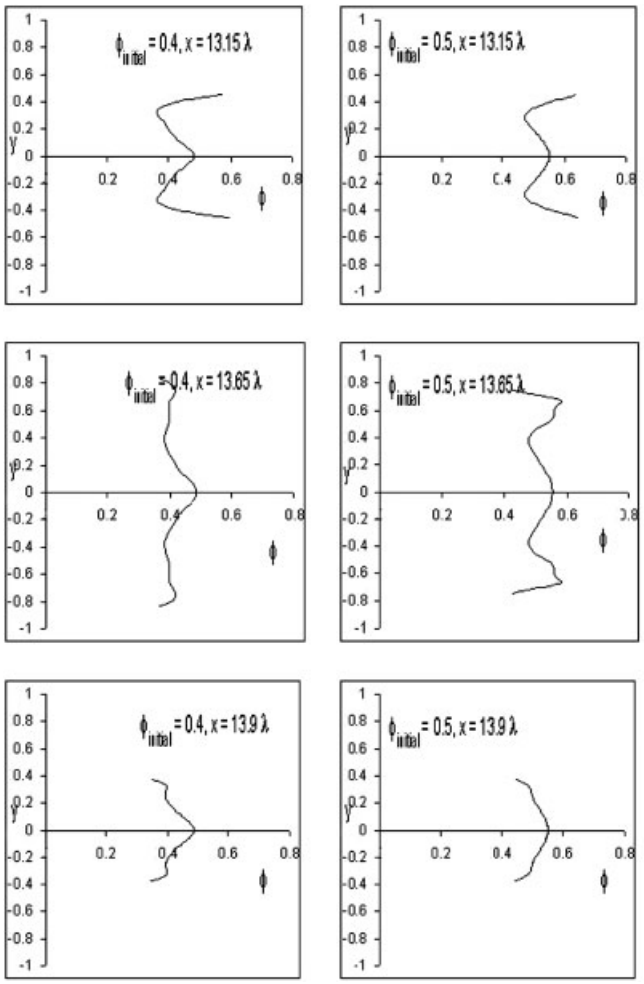

Figure 11. Concentration profiles of suspension flow for $Re = 300$.

$\phi_{\text{initial}} = 0.4$. It is interesting to note that for $Re = 120$ and $\phi_{\text{initial}} = 0.4$, this region is confined to only upstream section of wave 13 near the walls of the troughs of wave (Figure 12(b)). The higher concentration of the particles at the wall occurs at an axial location further upstream for $Re = 300$ than for $Re = 120$ when $\phi_{\text{initial}} = 0.4$ (Figure 12(a) and (b)). In addition, particle concentration at the wall in a small region where the channel height begins to decrease is close to the maximum packing fraction (Figure 11). This may be attributed to very low shear rate in this zone. The corresponding velocity profiles are presented in Figure 9 and are compared with the profiles for Newtonian model.

The contour plots for velocity and particle concentration when $Re = 300$ and $\phi_{\text{initial}} = 0.5$ are shown in Figure 13. In the region of minimum cross section, the shear rate at the wall is higher when $Re = 300$ and $\phi_{\text{initial}} = 0.5$ (Figure 14(b)) than when $Re = 120$ and $\phi_{\text{initial}} = 0.5$ (Figure 14(a)). This results in a strong migration of particles away from the wall towards the centreline of the geometry

DOI: 10.1002/fld

when $Re = 300$ and $\phi_{\text{initial}} = 0.5$ (Figure 13) at the inlet of the wave. The region further downstream is subjected to low velocities near the centreline region (Figure 9). The very low shear rates in the recirculation region (Figure 14(b)), which represents a region of low collisional frequency, lead to high particle concentration (closer to maximum packing fraction) in the wave troughs. This phenomenon is observed in the region closer to the wall where the channel height increases. A lower concentration at the wall in the centre of the wave is observed. Further downstream along the wall, the particle concentration again increases to a value close to maximum packing fraction (Figure 11). The particle concentration profiles gradually transform to their developing shape in the region of area reduction as one moves further downstream. The numerical results show that particles migrate from the regions of high shear zones and concentrate in the low shear zones and this behaviour is highly influenced by the values of Reynolds number and initial values of particle concentration.

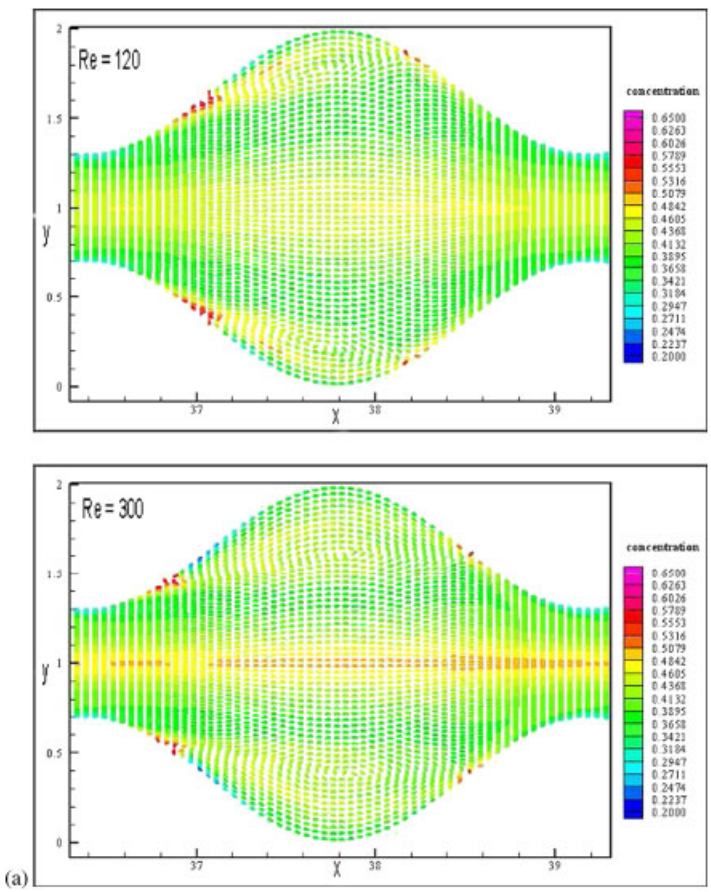

Figure 12. Contour plots for (a) concentration at $\phi_{\text{initial}} = 0.4$; (b) velocity at $\phi_{\text{initial}} = 0.4$; (c) shear rate for $\phi_{\text{initial}} = 0.4$; (d) pressure contours for the entire channel $\phi_{\text{initial}} = 0.4$; and (e) contour plots for pressure $\phi_{\text{initial}} = 0.4$.

DOI: 10.1002/fld

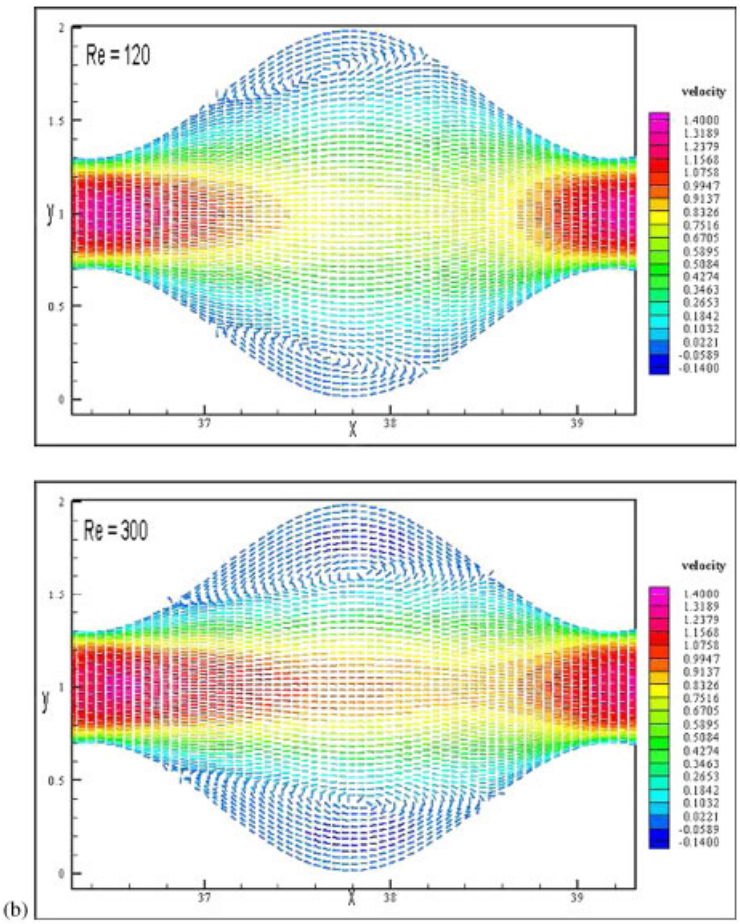

Figure 12. *Continued*.

It is interesting to observe that the velocity profile for concentrated suspension flow is blunted as compared with parabolic Newtonian flow as evident from Figures 8 and 9. Further, the blunting of velocity profile increases with increase in the particle concentration. It is worth mentioning here that such observations have also been made in the investigations on concentrated suspension Couette flow between eccentric rotating cylinders by Fang and Phan-Thien [33]. They have also observed a strong buildup of the particle volume fraction and a small recirculation zone in the wide gap of the Couette flow device (as observed in the present study for the case $Re = 300$ and $\phi_{\text{initial}} = 0.5$) at larger eccentricity ratios, leading to a significant change in the kinematics of the suspension due to the increase in effective viscosity. A similar observation has also been made in the investigation by Hofer and Perktold [34] for concentrated suspension flow in a stenosed tube. Their results show that, in the case of a stenosed tube model, particle concentration is lowest at the site of maximum concentration, whereas a strong accumulation of particles is observed in the recirculation zone downstream of the stenosis.

DOI: 10.1002/fld

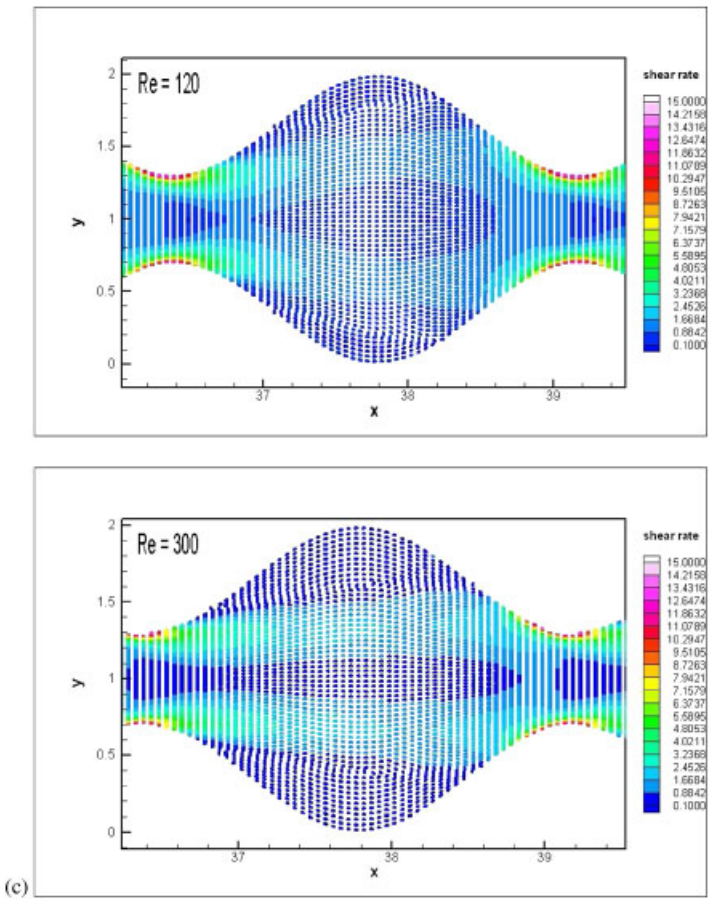

Figure 12. *Continued*.

5. CONCLUSIONS

The behaviour of concentrated suspensions containing neutrally buoyant spheres in a Newtonian liquid has been investigated using a finite volume method. A diffusive flux model is solved, which consists of Newtonian flow with a concentration-dependent viscosity and a diffusion equation for particle concentration. The diffusive fluxes depend on gradients of the shear rate, concentration and concentration-dependent viscosity. Thus, the suspension is modelled as a single continuum with the added effects of a particle concentration distribution.

The numerical computations in two-dimensional geometries such as a plane channel and a plane stenosed channel show non-uniform particle concentration distribution and blunted velocity profiles and these features captured by the model are consistent with the results from the diffusive flux model.

DOI: 10.1002/fld

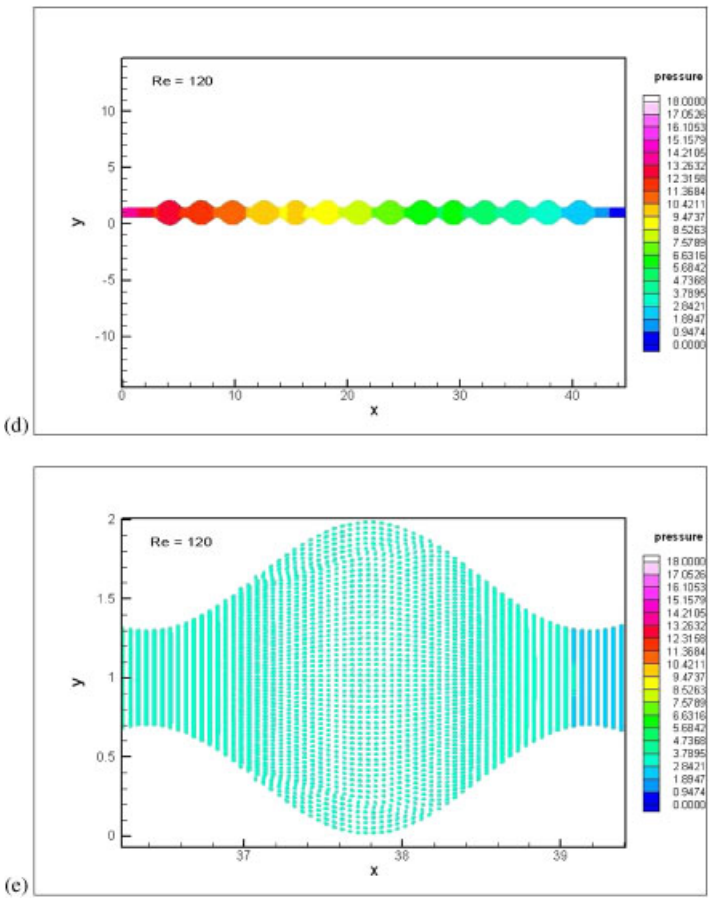

Figure 12. *Continued*.

The numerical results for a plane stenosed channel show that

- The particle concentration is lowest on the wall, at the site of maximum constriction as the area constriction results in high shear rates at the wall, which leads to a strong migration of particles away from the wall towards the inner section of the geometry.
- A strong accumulation of particles at the wall is observed in the recirculation zone downstream of the stenosis region because of the very low shear rates in the centre of the recirculation region.
- Recirculation in the regions downstream of the stenosis is suppressed by the particles. A blunting of the velocity profiles in the centreline region as compared with Newtonian flow without particles is observed.
- The maximum constriction percentage controls the behaviour of the particles. At lower constrictions (75% maximum area constriction), the flow is similar to plane channel flow and there are no recirculation zones. The particle distribution is similar to that in the plane channel geometry.

DOI: 10.1002/fld

The finite volume method has been effectively adapted to solve the flow in a wavy passage involving shear-induced particle migration in concentrated suspensions.

The numerical results show that

- The particles migrate towards regions of low shear rates with low velocities and thus form a near-stagnant region at these locations.
- The difference in computed particle concentration in the troughs of the wave close to the wall resulting from particle migration is found to increase at higher values of Reynolds number and more so with the increase in ϕ_{initial}.
- The velocity profile for the concentrated suspension flow is blunted as compared with the parabolic Newtonian flow.
- A recirculation region is observed in low Reynolds number flow ($Re = 120$) at $\phi_{\text{initial}} = 0.4$. The volume fraction attains a high value in a narrow region at the wall in the region of increasing cross section of the wave. For a higher value of ϕ_{initial} (0.5), the recirculation is

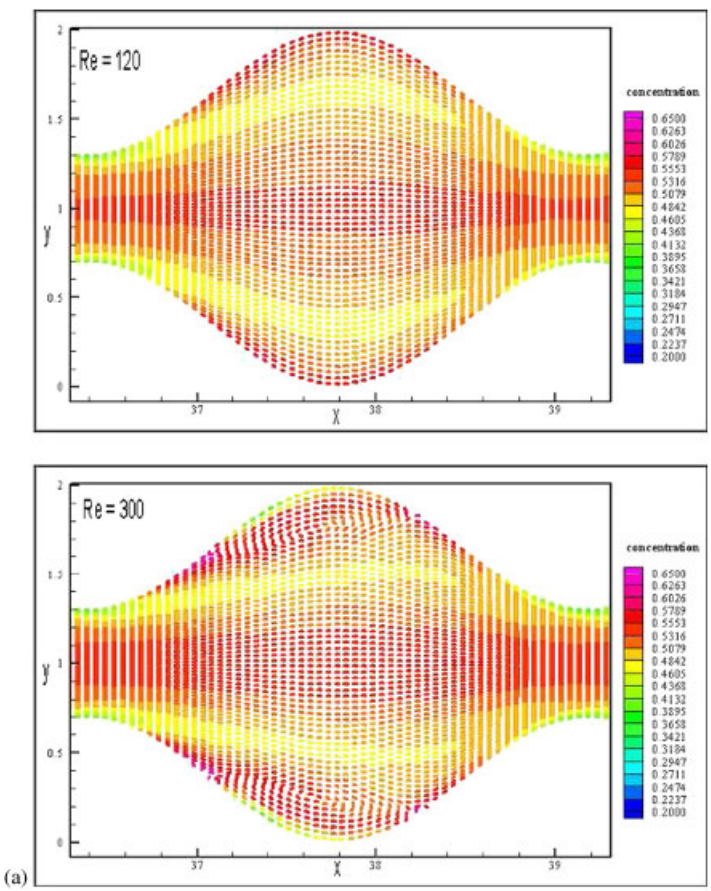

Figure 13. Contour plots for (a) concentration at $\phi_{\text{initial}} = 0.5$ and (b) velocity at $\phi_{\text{initial}} = 0.5$.

DOI: 10.1002/fld

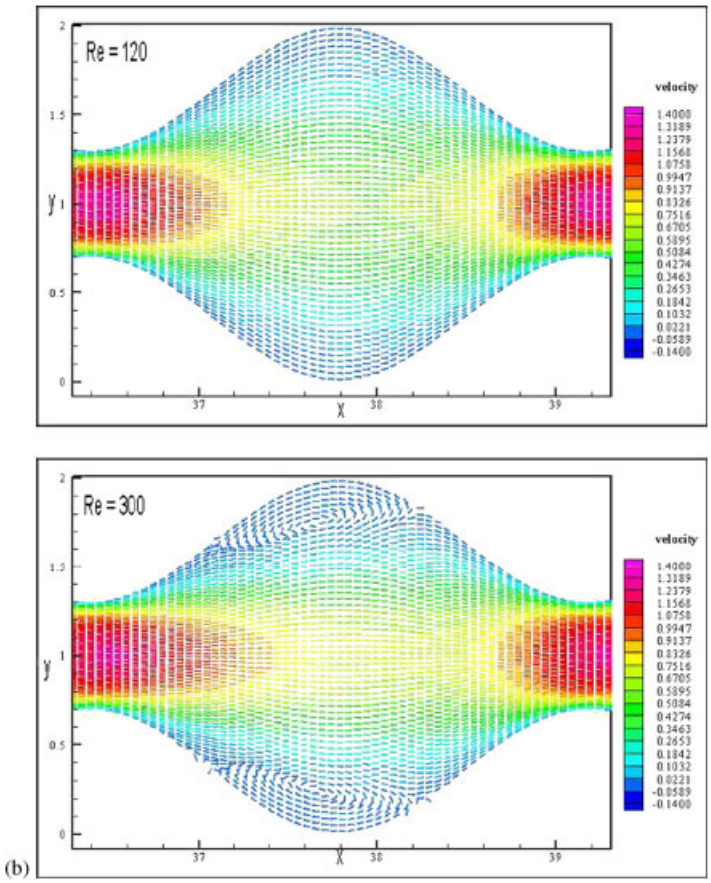

Figure 13. *Continued*.

found to be suppressed and no flow separation is visible. The particles accumulate at the walls of the troughs and at centreline giving rise to a high particle concentration in these regions. At higher Reynolds number ($Re = 300$), recirculation regions exist in troughs for all values of ϕ_{initial} (0.4 and 0.5).

The diffusive flux model incorporated into the finite volume method to investigate concentrated suspension flow in two-dimensional geometries in the present study describes the migration of particles within the suspension through a diffusion equation based on shear rate and effective viscosity gradients. However, this model lacks a complete description of the anisotropy of the particle interactions. A better model for suspensions should incorporate anisotropy, as it is one of the important characteristics of suspensions, which account for different amounts of resistance in flow fields.

A straight extension of the work will involve studying the flow for different parameters determining the shape of the wavy channel like the amplitude and wavelength.

It is worth mentioning that the present results may contribute to a better understanding of possible local variations of the particle concentration due to fluid–particle and particle–particle

DOI: 10.1002/fld

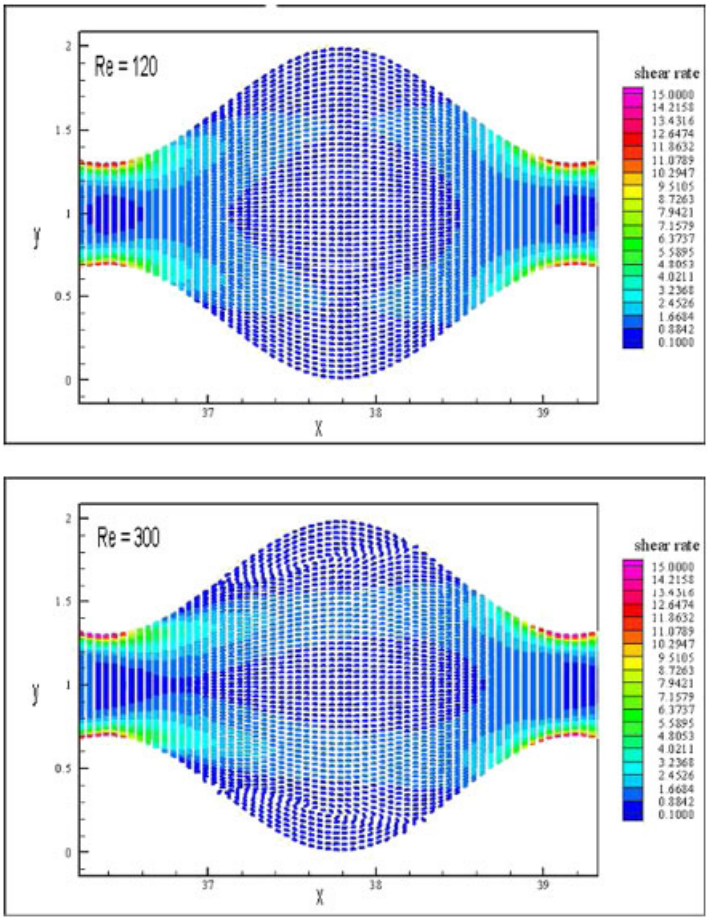

Figure 14. Contour plots of shear rate for $\phi = 0.5$.

interactions in certain applications, although the chosen values of parameters may be far from matching those in the applications where deformation and aggregation of the particles are essential factors and the particle size may be considerably smaller.

It is important to point out that issues such as onset of instabilities need to be examined since it is well established that non-Newtonian effects precipitate the onset of instabilities (experimental study of Kolodner [60]) and that wall corrugation promotes flow instabilities [61, 62] and these will be investigated in the future.

It is also of interest to obtain experimental data for the evolution of the particle velocity and concentration under the flow conditions similar to those considered in this study. The acquisition of these data is significant, since it would allow quantitative determination of the evolutionary state of results already present within the research literature and more importantly can be used to further test the quantitative applicability of the current model.

It is important to note that the present study has considered a suspension of rigid spheres in which migration effects are due to a phenomenon that is completely different from that which

DOI: 10.1002/fld

occurs in suspensions of deformable spheres (emulsions) and mammalian red blood cells. In view of this, the model predicts results that are far from reality of the blood circulation. Indeed, human blood is a concentrated suspension of highly deformable biconcave discs, able to change shape without significant expenditure of work, provided the membrane is not subject to an increase in surface area. Such deformations result in inward migration of red cells from the wall of tubes, as is found in emulsions of deformable drops. Moreover, at low shear rates, such as would prevail in certain areas of recirculation flow in sudden expansions of vessel diameter, red cells in plasma aggregate into so-called 'rouleaux'. Further, blunting of the velocity distribution occurs in the flow of human blood, but the effect is marked only at relatively low wall shear stress; as the shear stress increases and the deformation of the red cells increases, the blunting decreases until, at very high, flow and shear stress, the blunting disappears.

In view of the above, it is important to consider suspensions of deformable spheres and study the effects of particle migration in wavy passages and this forms a part of future investigation.

ACKNOWLEDGEMENTS

The authors sincerely thank the referees for their very valuable suggestions and useful comments. They have really improved the content, quality and style of the paper. They are also thankful for their suggestions about references on flows of non-Newtonian fluids in wavy passages. The authors also thank the editor Prof. Nigel Weatherill for his encouraging remarks and useful comments; Tata Consultancy Services for the use of its computational facilities at IIT Madras Computational Engineering Lab; and Dr Uma Balakrishnan, Center for Risk Studies and Safety, UCSB, CA for helping in the preparation of figures in this paper.

REFERENCES

1. Leighton D, Acrivos A. Measurement of shear-induced self-diffusion in concentrated suspension of spheres. *Journal of Fluid Mechanics* 1987; **177**:109–131.
2. Koh CJ, Hookham P, Leal LG. An experimental investigation of concentrated suspension flows in a rectangular channel. *Journal of Fluid Mechanics* 1994; **266**:1–32.
3. Cho YI, Kensey KR. Effects of the non-Newtonian viscosity of blood on flows in a diseased arterial vessel: part 1: steady flows. *Biorheology* 1991; **28**:241–262.
4. Liepsch D, Kamada T, Poll A, Morarec S. Two-phase flow measurements in glass tube models with a laser-doppler-anemometer. In *Recent Progress in Cardiovascular Mechanics*, Hosoda S, Yaginuma T, Sugawara S, Taylor MG, Caro CG (eds). Harword Academic Publishers: Chur, Switzerland, 1994; 21–47.
5. Perktold K, Resch M, Florian H. Pulsatile non-Newtonian flow characteristics in a three-dimensional human carotid artery bifurcation model. *Journal of Biomechanical Engineering—Transactions of the ASME* 1991; **113**:464–475.
6. Perktold K, Leuprecht A, Peter RO. Problems in application of viscoelastic models to the numerical analysis of arterial blood flow. In *Biofluid Mechanics*, *Proceedings of the 3rd International Symposium*, Munich, Liepsch D (ed.). VDI Reiche 17, vol. 107. VDI Verlag: Dusseldorf, 1994; 471–476.
7. Sharp MK, Thurston GB, Moore JE. The effect of blood viscoelasticity on pulsatile flow in stationary and axially moving tubes. *Biorheology* 1996; **33**:185–208.
8. Clifton RJ, Brown U, Wang JJ. Multiple fluids, proppant transport, and thermal effects in three-dimensional simulation of hydraulic fracturing. *Society of Petroleum Engineers Journal* 1988; 18198.
9. Unwin AT, Hammond PS. Computer simulations of proppant transport in a hydraulic fracture. *Society of Petroleum Engineers Journal* 1990; 29649.
10. Baree RD, Conway MW. Experimental and numerical modeling of convective proppant transport. *Society of Petroleum Engineers Journal* 1994; 28564.
11. Husband DM. Continuous processing of composite solid propellants. *Chemical Engineering Progress* 1989; **85**:55–61.

DOI: 10.1002/fld

12. Givler RC, Crochet MJ, Pipes RB. Numerical predictions of fiber orientation in dilute suspensions. *Journal of Composite Materials* 1983; **17**:330–343.
13. Leighton D, Acrivos A. Viscous resuspension. *Chemical Engineering Science* 1986; **41**:1377–1384.
14. Abbott JR, Tetlow N, Graham AL, Altobelli SA, Fukushima E, Mondy LA, Stephens TA. Experimental observations of particle migration in concentrated suspensions: Couette flow. *Journal of Rheology* 1991; **35**:773–794.
15. Arp PA, Mason SG. The kinetics of flowing dispersions. 9. Doublets of rigid spheres (experimental). *Journal of Colloid and Interface Science* 1977; **61**:44–61.
16. Gadala-Maria F, Acrivos A. Shear-induced structure in a concentrated suspension of solid spheres. *Journal of Rheology* 1980; **24**:799–811.
17. Goldsmith HL, Spain S. Radial distribution of white cells in tube flow. In *White Cell Mechanics*: *Basic Science and Clinical Aspects*, Meiselman HJ, Lichtman MA, Cokelet GR (eds). Alan R Liss Inc.: New York, 1984; 131–146.
18. Karnis A, Mason SG. The flow of suspensions through tubes. I. Meniscus effects. *Journal of Colloid and Interface Science* 1967; **23**:120–135.
19. Meiselman HJ. Some physical and rheological properties of human blood. *Sc.D. Thesis*, Massachusetts Institute of Technology, Cambridge, MA, 1965.
20. Chow AW, Sinton SW, Iwamiya JH, Stephens TS. Shear-induced migration in Coutte and parallel-plate viscometers: NMR imaging and stress measurements. *Physics of Fluids A* 1994; **6**:2561–2576.
21. Miskin I, Elliott L, Ingham DB, Hammond PS. Steady suspension flows into two-dimensional horizontal and inclined channels. *International Journal of Multiphase Flow* 1996; **22**:1223–1246.
22. Segre G, Silberberg A. Behaviour of macroscopic rigid sphere in Poiseuille flow, parts 1 and 2. *Journal of Fluid Mechanics* 1962; **14**:115–157.
23. Phillips RJ, Armstrong RC, Brown RA, Graham AL, Abbott JR. A constitutive equation for concentrated suspension that accounts for shear-induced particle migration. *Physics of Fluids A* 1992; **4**:30–40.
24. Hampton RE, Mammoli AA, Graham AL, Tetlow N, Altobelli SA. Migration of particles undergoing pressure-driven flow in a circular conduit. *Journal of Rheology* 1997; **41**:621–640.
25. Hookham PA. Concentration and velocity measurements in suspensions flowing through a rectangular channel *Ph.D. Thesis*, California Institute of Technology, New York, 1986.
26. Lyon MK, Leal LG. An experimental study of the motion of concentrated suspensions in two-dimensional channel flow. Part 1. Monodisperse systems. *Journal of Fluid Mechanics* 1998; **363**:25–56.
27. Buyevich IA. Particle distribution in suspension shear flow. *Chemical Engineering Science* 1996; **51**:635–647.
28. McTigue DF, Jenkins JT. Channel flow of a concentrated suspension. In *Advances in Micromechanics of Granular Materials*, Shen HH, Satake M, Mehrabadi M, Chang CS, Campbell CS (eds). Elsevier: Amsterdam, 1992; 381–481.
29. Mills P, Snabre P. Rheology and structure of concentrated suspensions of hard spheres: shear induced particle migration. *Journal of Physics*, *Part II* 1995; **2**:1597–1608.
30. Jenkins JT, McTigue DM. Transport processes in concentrated suspensions: the role of particle fluctuations. In *Two-phase Flows and Waves*, Joseph DD, Schaeffer DG (eds). Springer: New York, 1990; 70–79.
31. Nott PR, Brady JF. Pressure-driven flow of suspensions: simulation and theory. *Journal of Fluid Mechanics* 1994; **275**:157–199.
32. Zhang K, Acrivos A. Viscous resuspension in fully developed laminar pipe flow. *International Journal of Multiphase Flow* 1994; **20**:579–591.
33. Fang Z, Phan-Thien N. Numerical simulation of particle migration in concentrated suspensions by a finite volume method. *Journal of Non-Newtonian Fluid Mechanics* 1995; **58**:67–81.
34. Hofer M, Perktold K. Computer simulation of concentrated fluid–particle suspension flows in axisymmetric geometries. *Biorheology* 1997; **54**:261–279.
35. Sobey IJ. On the flow through furrowed channels. Part 1: calculated flow patterns. *Journal of Fluid Mechanics* 1980; **96**:1–26.
36. Stone K, Vanka SP. Numerical study of developing flow and heat transfer in a wavy passage. *Journal of Fluids Engineering—Transactions of the ASME* 1999; **121**:713–719.
37. Ahrens M, Yoo YJ, Joseph DD. Hyperbolicity and change of type in the flow of viscoelastic fluids through pipes. *Journal of Non-Newtonian Fluid Mechanics* 1987; **24**:67–83.
38. Pilitsis S, Beris AN. Calculation of steady-state viscoelastic flow in an undulating tube. *Journal of Non-Newtonian Fluid Mechanics* 1989; **31**:231–287.

DOI: 10.1002/fld

39. Beris AN, Avgousti M, Souvaliotis A. Spectral calculation of viscoelastic flows: evaluation of Giesekus constitutive equation in model flow problems. *Journal of Non-Newtonian Fluid Mechanics* 1992; **44**:197–228.
40. Pilitis S, Beris AN. Viscoelastic flow in an undulating tube. Part II. Effects of high elasticity, large amplitude of undulation and inertia. *Journal of Non-Newtonian Fluid Mechanics* 1991; **39**:375–405.
41. Pilitis S, Souvaliotis A, Beris AN. Viscoelastic flow in a periodically constricted tube: the combined effect of inertia, shear thinning and elasticity. *Journal of Rheology* 1991; **35**:605–646.
42. Davidson DL, Graessley WW, Schowalter WR. Velocity stress fields of polymeric liquids in a periodically constricted channel. Part I. Experimental methods and straight channel validations. *Journal of Non-Newtonian Fluid Mechanics* 1993; **49**:317–344.
43. Davidson DL, Graessley WW, Schowalter WR. Velocity stress fields of polymeric liquids in a periodically constricted channel. Part II. Observation of non-Newtonian behaviour. *Journal of Non-Newtonian Fluid Mechanics* 1993; **49**:345–375.
44. Ashrafi N, Khayat RE. A low-dimensional approach to nonlinear plane-Couette flow of viscoelastic fluids. *Physics of Fluids* 2000; **12**:345–365.
45. Abu Ramadan E, Khayat RE. Shear-thinning flow in weakly modulated channels. *International Journal for Numerical Methods in Fluids* 2005; **48**:467–499.
46. Rothstein JP, McKinley GH. Extensional flow of a polystyrene Boger fluid through a 4:1:4 axisymmetric contraction/expansion. *Journal of Non-Newtonian Fluid Mechanics* 1999; **86**:61–88.
47. Burdette SR, Coates PJ, Armstrong RC, Brown RA. Calculation of viscoelastic flow through an axisymmetric corrugated tube using the explicitly elliptic momentum equation formulation. *Journal of Non-Newtonian Fluid Mechanics* 1989; **33**:1–23.
48. Zheng R, Phan-Thien N, Tanner RI, Bush MB. Numerical analysis of viscoelastic flow through a sinusoidally corrugated tube using a boundary element method. *Journal of Rheology* 1990; **34**:79–102.
49. Abu Ramadan E, Khayat RE. On the interplay between inertial and viscoelastic effects for the flow in weakly modulated channels. *International Journal for Numerical Methods in Fluids* 2006; **51**:117–157.
50. Chiba K, Nakamura K, Boger DV. A numerical solution for the flow of dilute fiber suspensions through an axisymmetric contraction. *Journal of Non-Newtonian Fluid Mechanics* 1990; **35**:1–14.
51. Lipscomb II GG, Denn MM, Hur DU, Boger DV. The flow of fiber suspensions in complex geometries. *Journal of Non-Newtonian Fluid Mechanics* 1988; **26**:297–325.
52. Phan-Thien N, Fang Z. Entrance length and pulsatile flows of a model concentrated suspension. *Journal of Rheology* 1996; **40**:521–529.
53. Xue SC, Phan-Thien N, Tanner RI. Numerical study of secondary flows of viscoelastic fluid in straight pipes by an implicit finite volume method. *Journal of Non-Newtonian Fluid Mechanics* 1995; **59**:191–213.
54. Krieger IM. Rheology of monodisperse lattices. *Advances in Colloid and Interface Science* 1972; **3**:111–136.
55. Leighton D, Acrivos A. The shear-induced migration of particles in concentrated suspensions. *Journal of Fluid Mechanics* 1987; **181**:415–439.
56. Quemada D. Models of rheological behaviour of concentrated disperse media under shear. *Proceedings of IX International Congress on Rheology*, Mexico, 571–582.
57. Altobelli SA, Givler RC, Fukushima E. Velocity and concentration measurements of suspensions by nuclear magnetic resonance imaging. *Journal of Rheology* 1991; **35**:721–734.
58. Patankar SV. *Numerical Heat Transfer and Fluid Flow*. Hemisphere: New York, 1980.
59. Nishimura T, Ohoriand Y, Kawamura Y. Flow characteristics in a channel with symmetrical wavy wall for steady flow. *Journal of Chemical Engineering of Japan* 1984; **17**:466–471.
60. Kolodner P. Oscillatory convection in viscoelastic DNA suspensions. *Journal of Non-Newtonian Fluid Mechanics* 1998; **75**:167–192.
61. Floryan JM. Stability of wall bounded shear layers in the presence of simulated distributed surface roughness. *Journal of Fluid Mechanics* 1997; **335**:29–55.
62. Selvarajan S, Tulapurkara EG, Vasanta Ram V. Stability characteristics of wavy walled channel flows. *Physics of Fluids* 1999; **11**:579–589.

DOI: 10.1002/fld